Design of Dual Band-Reject Filter based on Short-Circuited Parallel Coupled Lines Structure at S-Band

Salman Raju Talluri

Department of Electronics and Communications Engineering
Jaypee University of Information Technology, Solan, Himachal Pradesh, India
salmanraju.talluri@juit.ac.in

Abstract: This paper presents a simple design of dual-band reject filter based on parallel coupled lines structure. Parallel coupled lines structure is a four-port network. A dual-band shunt resonator using this structure is obtained by short-circuiting two opposite ports to ground and connecting one of the two remaining ports to a transmission line in shunt. The fourth port is an open circuit. This modified parallel coupled lines structure has been connected with a high impedance transmission line to obtain the narrow dual band reject filter. Theoretical analysis has been performed in order to obtain the resonant frequencies. The numerical simulations have been performed and these results have been verified by the full-wave electromagnetic simulations for an S-band dual band reject filter with rejecting frequencies at 2.5 GHz and 3.5 GHz. The control over the band rejection frequencies is obtained by selecting the parameters of the parallel coupled lines in terms of gaps, widths, and lengths.

Keywords: Dual band reject filter, parallel coupled lines, stub, transmission line theory.

1. Introduction

Design of multi-bandpass/band reject filters has gained a lot of attention in recent days [1-3]. Different types of techniques have been proposed to design dual-bandpass/band reject filters [4-5]. Based on interdigital hairpin structure a tri-bandpass filter has been proposed [6]. Along with these there are stepped impedance resonators, defected ground structure resonators [7]. Using the composite right/left-handed resonators, ultra-wideband bandpass filter has been designed with dual notch bands [8]. Recently, compact balance dual bandpass filter based on coupled embedded resonators have been presented [9]. After this, multi interference suppression capability has been reported [10]. Dual band stop filters have been also proposed using the parallel coupled lines by introducing transmission zeros [11-14]. All these methods are based on the properties of the stubs and these designs are not using the coupling between the parallel lines.

This paper completely depends on the coupling characteristics of two parallel coupled lines structure [15]. Since the parallel coupled lines structure has two degrees of freedom in terms of widths and gaps between the lines, it is possible to have a dual-band resonator with slight modifications in the parallel coupled lines structure. The coupling property has been used in this paper to design a dual-band reject filter.

This paper presents the theoretical analysis, followed by numerical analysis and finally the full-wave electromagnetic simulations. The proposed theory is verified by the full wave electromagnetic simulations with reasonable deviations from the numerical simulations.

2. Problem Formulation

The proposed dual-band reject resonator based on parallel coupled lines structure is shown in Figure 1. Every transmission line section is periodic depending on the length of the transmission line section. In the same manner, a parallel coupled lines structure is also periodic. Usually transmission lines and parallel coupled lines structures are periodic with half wavelength. In electrical length terms, it is equal to π radians.

In order to observe the proposed structure frequency characteristics over a period (π radians), it is required to observe the scattering parameters. A parallel-coupled lines structure is characterized by even mode (z_e) and odd mode impedances (z_o). The characteristic impedance of the parallel coupled lines structure (z_c) is generally considered as the average of even mode and odd mode impedances. These even mode impedance and odd mode impedances depend on width (W_c) and gap (S) between the parallel coupled lines structure.

Two parallel coupled lines form a four port network as shown in Figure 2. It is represented by impedance parameters in terms of even mode impedance and odd mode impedance [16].

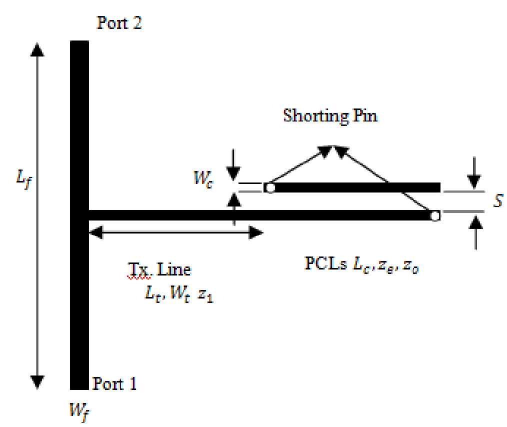

Fig.1 Microstrip layout of the proposed structure.

DOI: http://dx.doi.org/10.32452/IJAMT.2018.180184

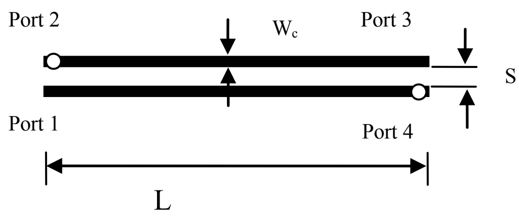

Fig.2 Parallel coupled lines structure with short circuits.

$$z_{11} = z_{22} = z_{33} = z_{44} = -\frac{j}{2}(z_e + z_o)\ \cot\theta \qquad (1)$$

$$z_{12} = z_{21} = z_{34} = z_{43} = -\frac{j}{2}(z_e - z_o)\ \cot\theta \qquad (2)$$

$$z_{13} = z_{31} = z_{24} = z_{42} = -\frac{j}{2}(z_e - z_o)\ \csc\theta \qquad (3)$$

$$z_{14} = z_{41} = z_{23} = z_{32} = -\frac{j}{2}(z_e + z_o)\ \csc\theta \qquad (4)$$

Here θ is the electrical length of the parallel coupled lines. Electrical length at an operating frequency (expressed in wavelength) is defined as $\theta = \beta L = \frac{2\pi}{\lambda}L$. The physical length L is usually expressed in terms of wavelength so that the product of β and L will be in radians independent of the frequency of operation and the physical length of the line.

Since the proposed structure in Fig.1 has two shorting pins (With microchip technology, shorting pin is obtained by drilling the top layer of the printed circuit board with the trace and providing a metallic contact of the top layer with the bottom ground layer), it is required to find the input impedance of the modified parallel coupled lines structure with conditions given in Eqn.5. Fig.2 represents the port notations of the parallel coupled lines structure and with respect to these port numbers, the following conditions are required to be incorporate in the calculation of input impedance.

$$v_2 = 0, v_4 = 0\ and\ i_3 = 0 \qquad (5)$$

After incorporating these conditions, the input impedance of parallel coupled lines structure at port 1 with the above constraint is obtained as:

$$z_{in} = z_{11} - z_{12}\frac{z_{11}z_{12} - z_{13}z_{14}}{z_{11}^2 - z_{13}^2} - z_{14}\frac{z_{11}z_{14} - z_{12}z_{14}}{z_{11}^2 - z_{13}^2} \qquad (6)$$

In order to obtain the resonant frequencies, the input impedance of this modified parallel coupled line has been equated to zero, so that the band rejection frequencies can be obtained for the proposed structure. This is simply obtained by equating the denominator of Eq.6 to zeros. The resonant frequencies are obtained from this as:

$$\theta_{r1} = \tan^{-1}\left(\frac{2\sqrt{z_e z_o}}{z_e - z_o}\right)\ and\ \theta_{r2} = \pi - \tan^{-1}\left(\frac{2\sqrt{z_e z_o}}{z_e - z_o}\right) \qquad (7)$$

From Eq.7, it is observed that there are two frequencies for a given set of even and odd mode impedances. This formula is valid only for a simple section of parallel coupled line structure shown in Figure 2. The main advantage of this equation is the generation of two frequencies at which the return loss of this structure is zero. It is not possible to obtain two resonant frequencies with a simple transmission line stub either with an open circuit or short circuit.

This modified parallel coupled lines structure has been connected to a transmission line of length L_t with a characteristic impedance of z_1. It is assumed that if the width of the parallel coupled line is same as that of this transmission line, both the characteristics impedances are same, i.e. the characteristic impedance of the transmission line is exactly same as that of the characteristic impedance of the parallel coupled line.

Since this parallel coupled lines structure is connected to a transmission line, this circuit acts as a load for the transmission line. Using the standard formula for finding the input impedance of a transmission line terminated with load impedance, the overall input impedance can be obtained. From this, it can be found out the transmission zeros. These resonant frequencies will be shifted slightly in respect to Eqn.7. It is little difficult to obtain the closed loop expressions for these resonant frequencies. However, there will be still two transmission zeros in the entire periodicity. This now can be connected in the main line of the transmission line (feed line) so that it can be connected in shunt. And finally, it is required to find the scattering parameters of the two-port network in order to observe its frequency characteristics.

3. Numerical Simulations

Numerical simulations have been performed with normalized impedances in terms of electrical length θ. The length of the parallel coupled lines structure is taken as unity, same as that of a high impedance transmission line. In order to verify the numerical simulation by the full wave electromagnetic simulations, some set of practically realizable values of the parallel coupled lines structure has been considered in terms of widths and gaps. The considered values for the proposed layout in Fig.1 have been tabulated in Table 1. The impedance values for these physical dimensions on the substrate of FR-4 ($\epsilon_r = 4.3$) with a thickness of substrate 1.6 mm that will give electrical properties of characteristic impedance, even and odd mode impedances are shown in the same table.

These values are obtained by a transmission line calculator provided by National Instruments [17]. Matlab [18] is used for numerical simulations.

Table.1 Values of even mode and odd mode impedances for different widths and gaps of PCLs structure.

S.No.	Parameter (mm)	Impedance (Ohms)	Normalized Values with respect to z_f
1	$W_c = 0.95$	$z_c = 88.688$	1.503
2	$W_f = 2.3$	$z_f = 59.002$	1
3	$W_c = 0.95$ $S = 0.55$	$z_e = 117.491$ $z_o = 59.525$ $z_c = 88.508$	2 1.008 1.5
4	$W_c = 0.95$ $S = 0.35$	$z_e = 121.194$ $z_o = 53.300$ $z_c = 87.247$	2.054 0.903 1.478
5	$W_c = 0.65$ $S = 0.75$	$z_e = 136.66$ $z_o = 74.078$ $z_c = 105.369$	2.316 1.255 1.785

DOI: http://dx.doi.org/10.32452/IJAMT.2018.180184

Figure 3 represents the scattering parameters of the single section parallel coupled transmission lines structure for Row-3 of Table.1. The same figure has a comparison with open-circuited stub and short-circuited stub which can only introduce a single pole or zero. The values shown in this figure can also be obtained using Eq.7. Since this structure cannot be directly connected to the feed line, a small section of the high impedance transmission line is connected and its effects are observed for three different lengths. Figure 4 represents the variation of scattering parameters for three connecting line lengths. From this figure, it is observed that there is a small change in the center frequency around $\pi/2$ while at higher electrical lengths this effect can be felt. In order to have a periodicity (the smallest length in the geometry decides the periodicity), the length of the connecting section has been taken as equal to the parallel coupled line structure as shown in Figure 1.

Figure 5 represents the frequency response of the proposed structure with normalized values of impedances (from Row-3 to Row-5) shown in Table.1. It is observed from this figure, the periodicity of the structure is π radians while the rejection frequencies are near $\pi/2$.

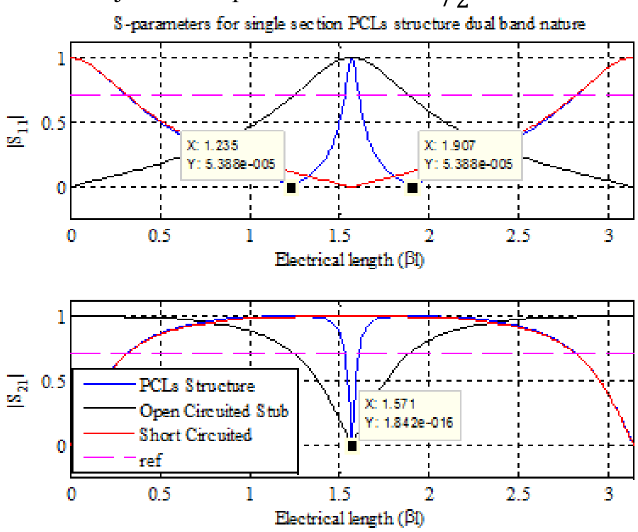

Fig.3 Single section parallel coupled lines structure with short circuits.

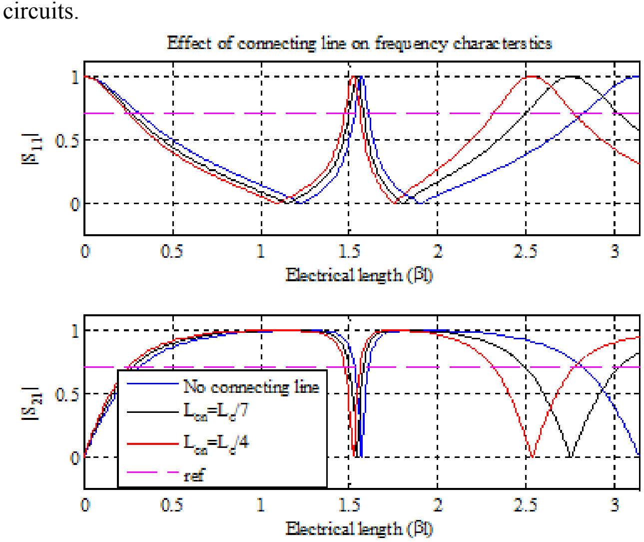

Fig.4 Effect of connecting line on parallel coupled lines structure with short circuits.

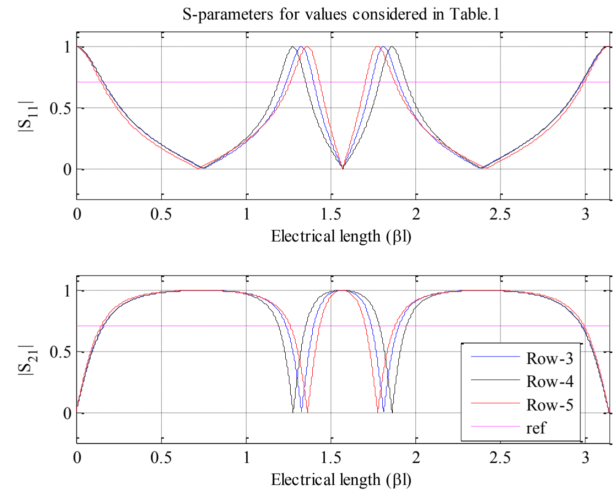

Fig.5 Frequency response of the proposed structure with respect to values considered in Table.1

These frequencies are symmetric about $\pi/2$. Figure 6 is an enlarged version of the Figure 5 in order to represent the resonant frequencies of the structure for three different values of impedance configurations as shown in Table1 for Row-3 to Row-5. These values can be used to verify the full-wave electromagnetic simulations. If it is required to design a dual-band reject filter symmetrically about 3 GHz, then $\pi/2$ radians must be scaled to 3 GHz. If this has scaled to 3 GHz, then 1.329 radians must correspond to a value of 2.5382 GHz and 1.813 radians must be proportional to 3.4625 GHz. If the full-wave electromagnetic simulation results are within the proximity of these values, then the numerical simulations and full-wave electromagnetic simulations are verified. Similarly, for other values, the corresponding frequencies can be obtained. For 1.279 radians, the frequency is 2.4427 GHz and for 1.862 radians, the frequency is 3.5561 GHz. For 1.363 radians, the frequency is 2.6031 GHz while for 1.778 radians, the frequency is 3.3957 GHz. From this figure, it is observed that in order to control the rejection band frequencies, the design parameters that must be varied are the width and gap of the parallel coupled lines structure.

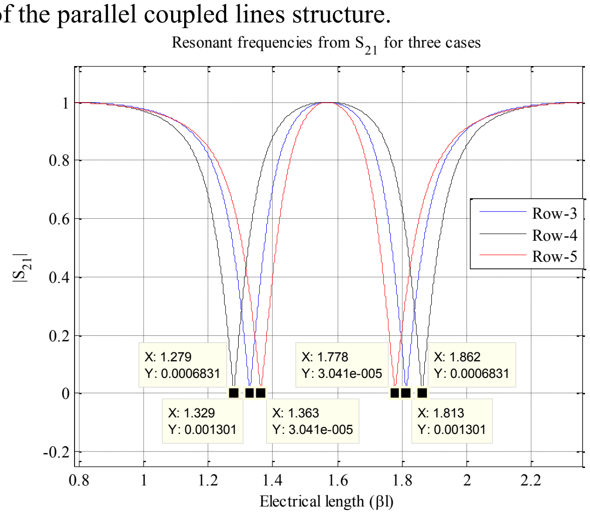

Fig.6 Enlarged view of resonant frequencies for three cases considered in Table.1

DOI: http://dx.doi.org/10.32452/IJAMT.2018.180184 © 2018 IJAMT

4. Full-wave simulations and results

With the values considered in Table1, the microstrip layout is obtained and all the details of the simulated structure are presented in Table 2. The lengths of the transmission line and parallel coupled lines structure are taken as 14.0 mm. This corresponds to a center frequency of 3.0 GHz on the considered substrate.

Figure 7 represents the frequency characteristics of the single section with a connecting line of length 0.2 mm. The actual length of the parallel coupled lines structure is 14.0 mm. As mentioned from the numerical simulations, this has the effect of shifting the resonant frequency to lower frequencies. This has been verified from the full wave simulations as well since the resonant frequency now appearing at 2.796 GHz.

Figure 8 represents the frequency characteristics of the proposed structure as a single section and two similar cascaded sections. From this graph, the resonant frequencies are obtained at 2.487GHz and 3.465 GHz for a single section and for two similar cascaded sections; it is again at almost same frequencies of 2.481 GHz and 3.456 GHz. The cascaded section has been considered to improve the roll-off of the filter. The separation between these two cascaded sections is again 14.0 mm. According to numerical simulations, the value of 2.487 GHz must be at 2.538GHz and 3.465 GHz should have been at 3.462GHz. Since these values are almost matching with numerical simulations, the proposed design is verified.

Table.2 Dimensions of the microstrip layout for band rejection frequencies of 2.5 GHz and 3.5 GHz

S.No.	Parameter	Value
1	Length of feed line (L_f)	10 mm
2	Length of Tx line stub (L_t)	14 mm
3	Length of PCL section (L_c)	14 mm
4	Width of feed line (W_f)	2.3 mm
5	Width of PCL section (W_c)	0.95 mm
6	Spacing between PCLs (S)	0.55 mm
7	Height of the substrate (H)	1.6 mm
8	Thickness of copper cladding (T_c)	0.035 mm
9	Radius of shorting pin (r)	0.2 mm

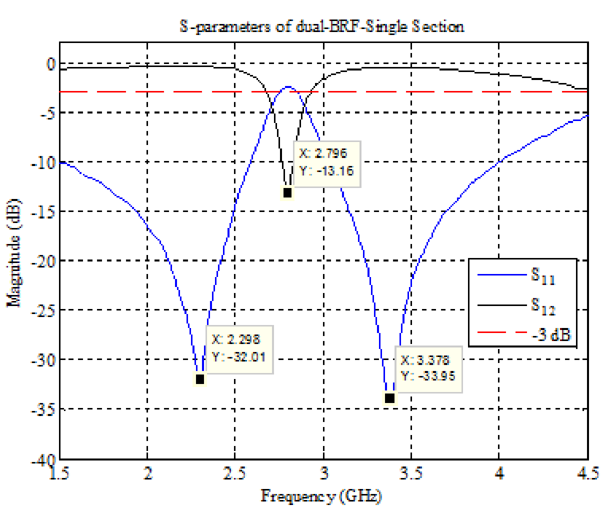

Fig.7 Single section parallel coupled lines structure with short circuits as Row-3 of Table.1.

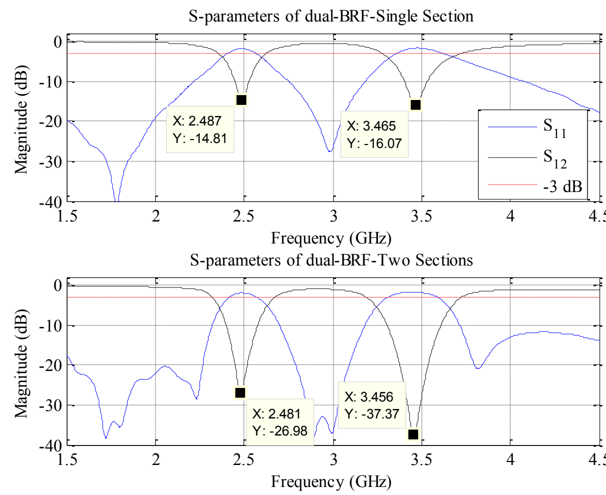

Fig.8 Frequency response of single and cascaded sections of dual-band reject resonator.

Figure 9 represents the frequency characteristics of the remaining two rows (Row-4 and Row-5) of Table 1. Again from this figure, it is observed that for a gap of S=0.35 mm and width of W=0.95 mm (Row-4), the resonant frequencies are 2.397 GHz and 3.57 GHz from full-wave simulations and from numerical simulations, these values correspond to 2.442 GHz and 3.556 GHz. Similarly, for a gap of S=0.75 mm and W=0.65 mm, the resonant frequencies are 2.586 GHz and 3.465 GHz. According to numerical simulations, these values have been proportional to 2.603 GHz and 3.395 GHz. From all these simulations, the full wave simulations are very close to the numerical simulations which validate the design of dual-band reject filter.

Finally, the length of the parallel coupled lines structure has been varied for two gaps (S) with the same widths. Fig.10 represents the variation of resonant frequencies for two lengths for a gap of 0.55 mm and 1.1 mm. From this figure, it is observed that the center resonant frequency (in this case 3 GHz) can be altered by changing the length of the proposed structure. In order to have asymmetry in the rejection frequencies, the spacing can be altered.

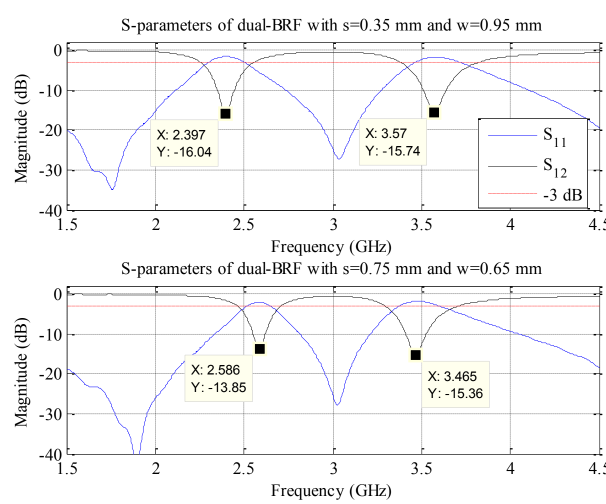

Fig.9 Frequency response of single section dual band reject resonator with different widths and separations.

DOI: http://dx.doi.org/10.32452/IJAMT.2018.180184

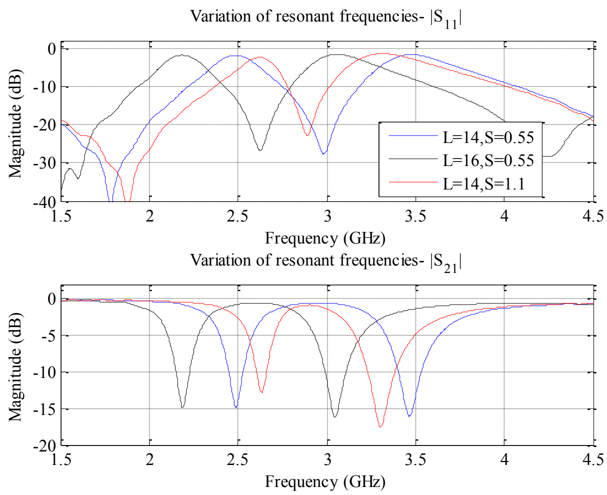

Fig.10 Frequency response of single section dual band reject resonator with different separations and lengths.

The main application of this structure is to reject two nearby frequencies. The main limitation of this structure is the proper selection of the physical parameters of the layout.

5. Conclusion

A simple dual-band reject resonator based on parallel coupled lines structure has been proposed. Using this resonator, a dual-band reject filter rejecting at 2.5 GHz and 3.5 GHz has been designed. This design has been validated by numerical simulations and full-wave electromagnetic simulations. This paper also presented the control of the resonant frequencies by varying the design parameters of the structure in terms of gap, width, and lengths of the parallel coupled lines structure.

References

[1] Y. Mehmet, A reconfigurable microwave combine filter, *IEEE Transactions on Circuits and Systems II: Express Briefs,* vol. 63, no.1, pp.84-88, 2016.

[2] W.-J Zhou and J. X. Chen, High-selectivity tunable balanced bandpass filter with constant absolute bandwidth, *IEEE Transactions on Circuits and Systems II: Express Briefs,* vol. 64, no.8, pp. 917-921, 2017.

[3] W. Feng, Y. Zhang, and W. Che, Tunable dual-band filter and diplexer based on folded open loop ring resonators, *IEEE Transactions on Circuits and Systems II: Express Briefs,* vol. 64, no.9, pp. 1047-1051, 2017.

[4] Hong, Jia-Sheng, Microstrip dual-mode band reject filter, *Microwave Symposium Digest, 2005 IEEE MTT-S International*. IEEE, 2005.

[5] Awida, A. Balalem, A.M.E. Safwat, H.M. EL-Hennawy, and A. Omar, Combined low-pass and bandpass filter response using microstrip dual-mode resonators, *Microwave Symposium Digest, 2006. IEEE MTT-S International,* pp. 702-704, 2006.

[6] Wang, F. Nasri, and C.-W. Park, Compact tri-band notched UWB bandpass filter based on interdigital hairpin finger structure, Wireless and Microwave Technology Conference (WAMICON), 2011 IEEE 12th Annual. IEEE, 2011.

[7] Hong, Jia-Shen G., and Michael J. Lancaster. *Microstrip filters for RF/microwave applications*. Vol. 167. John Wiley & Sons, 2004.

[8] F. Wei, Q.Y. Wu, X.W. Shi, and L. Chen, Compact UWB bandpass filter with dual notched bands based on SCRLH resonator." *IEEE Microwave and wireless components Letter,* vol. 21, pp. 28-30, 2011.

[9] F. Bagci, A. F. Prieto, A. Lujambio, J. Martel, J. Bernal, and F. Medina, Compact balanced dual-band bandpass filter based on modified coupled-embedded resonators, *IEEE Microwave and Wireless Components Letters,* vol. 27, no.1, pp. 31-33, 2017.

[10] D. Psychogiou, R. G. García, and D. Peroulis, RF wide-band bandpass filter with dynamic in-band multi-interference suppression capability, *IEEE Transactions on Circuits and Systems II: Express Briefs,* vol. 65, no. 7, pp. 898-902, 2018.

[11] G. Liu, and Y. Wu, Novel in-line microstrip coupled-line bandstop filter with sharp skirt selectivity, *Progress In Electromagnetics Research*, vol. 137, pp.585-597, 2013.

[12] J. –Y. Shao and Y.-S. Lin.,Narrowband coupled-line bandstop filter with absorptive stopband, *IEEE Transactions on Microwave Theory and Techniques*, vol. 63, no.10, pp. 3469-3478, 2015.

[13] W. J. Feng, M.J. Hong, W.Q. Che, and Q, Xue, Dual-band microstrip bandstop filter with multiple transmission poles using coupled lines, *IEEE Microwave and Wireless Components Letters*, vol. 27, no.3, pp.236-238, 2017.

[14] J. M. Yan, L.Cao, and H.-Y. Zhou, A novel quad-band bandstop filter based on coupled-line and shorted stub-loaded half-wavelength microstrip resonator, *Progress In Electromagnetics Research*, vol. 79, pp. 65-70, 2018.

[15] S. B. Cohn, Parallel-coupled transmission-line-resonator filters, *IRE Transactions on Microwave Theory and Techniques,* vol. 6, no. 2, pp.223-231, 1958.

[16] D.M. Pozar, *Microwave Engineering,* John Wiley & Sons, 2009.

[17] https://www.awrcorp.com/products/additional-products/tx-line-transmission-line-calculator.

[18] MathWorks, MATLAB: the Mathworks Inc., Natick, MA(2010).

Biography of the authors

Salman Raju Talluri has completed his M.Tech from IITK in 2009 and obtained his Ph.D. titled "Analysis of non-linear transmission lines for opposite phase and group velocities" in 2017 from Jaypee University of Information Technology, Solan, Himachal Pradesh, India. His areas of interest include non-linear transmission lines, microwave engineering, and antenna arrays. He is currently working as an assistant professor at the Jaypee University of Information Technology, Solan. He was with the Astra microwave products limited, Hyderabad for one year from 2006 to 2007.